TEVATRON RUN II LUMINOSITY, EMITTANCE AND COLLISION POINT SIZE

J. Slaughter, J. Estrada, K. Genser, A. Jansson, P. Lebrun, J. C. Yun,

Fermi National Accelerator Laboratory, Batavia, IL 60510,

S. Lai,

University of Toronto, Toronto, Canada M5S 1A7

Abstract

We compare the Tevatron luminosity as measured by the CDF and D0 experiments with that computed from machine characteristics. We also compare the CDF measurements of the size of the interaction region with that predicted by machine parameters. Although these results are still preliminary, they show promise as a useful crosscheck of the instrumentation and our understanding of the Tevatron machine characteristics.

INTRODUCTION

Understanding the behavior of the Tevatron depends on understanding the instrumentation and the lattice parameters. The experiments D0 and CDF provide independent measurements of the luminosity[1] and of the size of the luminous region. The luminosity (10^{30}cm^{-2}sec^{-1}) can also be calculated from lattice parameters and beam measurements in the Tevatron, as

$$L = \frac{10^{-5} f B N_p N_{\bar{p}} (6\beta_r \gamma_r)}{2\pi\beta^* \sqrt{(\varepsilon_p + \varepsilon_{\bar{p}})_x (\varepsilon_p + \varepsilon_{\bar{p}})_y}} H(\sigma_l / \beta^*). \quad (1)$$

Here, N_p and $N_{\bar{p}}$ are the numbers of protons and anti-protons per bunch (~10^9), B is the number of bunches (36), f is the revolution frequency (47.7 KHz) and $\beta_r\gamma_r$=1045 is the relativistic factor, β^* is the beta function at the interaction point (measured in cm, and assumed equal in x and y). H is the hourglass factor, a function of the bunch length σ_t and β^*, and finally ε_p and $\varepsilon_{\bar{p}}$ are the proton and anti-proton 95% normalized emittances in π-mm-mr. Comparing the calculated luminosity to the measured one provides a crosscheck between the Tevatron beam instrumentation and the detectors.

The experiments very accurately measure the size of the luminous regions at the interaction points as a function of z (distance along the beam axis) from the distributions of primary vertices as measured by the silicon vertex detectors. In the simplest model,

$$\sigma(z) = \sqrt{\varepsilon\left(\beta^* + (z - z_0)^2 / \beta^*\right)}, \quad (2)$$

where σ is the rms beam size, $\varepsilon = (\varepsilon_p \varepsilon_{\bar{p}})/((\varepsilon_p + \varepsilon_{\bar{p}})$ is a pseudo-emittance and z_0 is the z location where β is a minimum. Note that if the p and pbar emittances are equal, the pseudo-emittance is half the equivalent beam emittance.

Although not discussed in this paper, CDF can measure the bunch lengths of the p and pbar bunches separately by using the Central Outer Tracker (COT) information in conjunction with the time of flight (TOF) system[2].

SIZE OF THE LUMINOUS REGIONS

CDF has fit for ε, β^* and z_0 in Equation 2 for 20 runs in 14 stores from the last 6 months of 2002. Figure 1 shows typical distributions for one run with fits to Equation 2. The average values of the parameters are given in Table 1. The average β^* is 38 cm, 9% larger than the nominal 35 cm and the minimums are displaced with respect to the center of CDF. It is expected that β^* and z_0 are the same store to store, but not ε. Fixing β^* to the average β^*, 38.6 cm in x and 38.0 in y, and then refitting improves the fits, while fixing β^* to the nominal 35 cm gives slightly worse fits. The average over 20 runs of the run-by-run ratio of x and y pseudo-emittances is 1.01±.04. If the proton and anti-proton emittances are assumed to be the same*, then the pseudo-emittances imply that their values are 15.7±1.5 π-mm-mr in the horizontal plane and 15.8±1.5 π-mm-mr in the vertical plane. The largest uncertainties in the vertex measurements are, first, that they integrate over a significant time period, ranging from 4 to 15 hours with an average of 8 hours, in which the emittances are changing, and, second, they rely on proper subtraction of the measurement resolution. In this preliminary analysis the experimental resolution that is subtracted in quadrature from the uncorrected beam width is about equal to the resulting beam width.

* The flying wires give a ratio of anti-proton to proton emittance of 1.00±.22 in the horizontal plane and 1.03±.13 in vertical plane, based on data from 95 stores.

This works was supported by Department of Energy of the U.S. under contract no DE-AC002-76CH03000 and by the Natural Sciences and Engineering Research Council of Canada.

Table 1 Luminosity weighted averages over 20 runs from fits to Equation 2. The errors are the weighted standard deviations. The emittances ε_x and ε_y are pseudo-emittances as defined in the text. The column labeled equivalent emittance is obtained by inverting $\varepsilon = (\varepsilon_p \varepsilon_{\bar{p}})/2(\varepsilon_p + \varepsilon_{\bar{p}})$, assuming the proton and anti-proton emittances are the same.

	β_x (cm)	β_y (cm)	ε_x π-mm-mr	ε_y π-mm-mr	Z_{0x} (cm)	Z_{0y} (cm)	equivalent emittance π-mm-mr
β_x, β_y free	38.6±2.5	38.0±3.0	7.9±1.1	7.8±1.0	14.2±1.6	-9.2±1.7	15.7±1.5
β_x, β_y fixed	38.6	38.0	8.0±1.1	7.9±1.1	14.3±3.1	-9.2±1.4	15.8±1.5
β_x, β_y fixed	35.0	35.0	8.3±1.2	8.1±1.2	13.3±1.1	-8.5±1.4	

LUMINOSITY DETERMINATIONS

Using Equation 1, we compare the luminosities as measured by CDF and D0 with the calculated luminosities. The intensities are measured using the FBIs (Fast Bunch Integrator)[3], The hourglass factor is calculated using the bunch length σ_t from the SBD (Sampled Bunch Display)[4] and the emittances are measured by either the flying wire system (FW)[5] or the synchrotron light (SL) system[6]. Since the flying wires cause background for the experiments, they are only flown once at the beginning of the store and then again at the end, just before terminating the store. The SL measurements are made continuously throughout the HEP store.

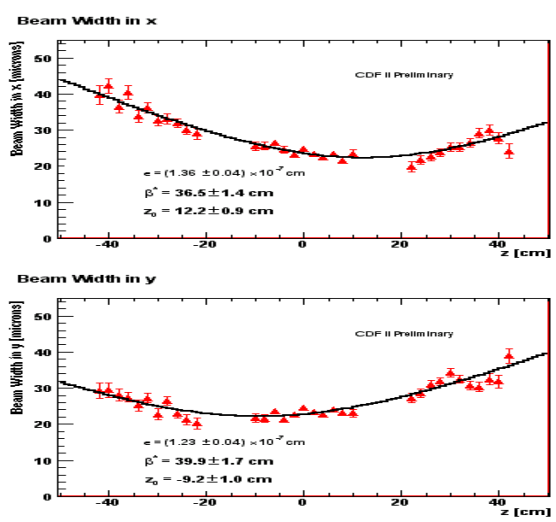

Figure 1 Example plot for one run of 20 runs showing luminous region size versus z and the fits to Equation 2. Typical correlation coefficients of the fits are about -0.8 for (β^*, ε), 0.5 for (β^*, z_0), and -0.6 for (ε, z_0)

Figure 2 plots the ratio of the bunch-by-bunch calculated luminosity to the CDF luminosity at the beginning of the store as a function of CDF luminosity for a sample of 52 recent stores. The calculated luminosity uses the FW emittances. Figure 3 shows the same ratio but for D0, using 5 stores. Each store has approximately 100 measurements taken every 10 minutes. The calculated luminosity uses the SL emittances and assumes that the horizontal emittance equals the vertical one for p and pbar respectively. The main characteristic of the plots is a systematic scale factor that is a function of luminosity, although with different intercepts and slopes. In Figure 2 the slope is -0.22±0.03 and the intercept is 0.92±.02(Fit 1). In Figure 3, the slope is –0.0634±0.0002 and the intercept is 0.7702±0.0003(Fit 2). The equivalent analysis but for CDF, gives –0.0826±0.0012 and 0.7455±0.0008(Fit 3).

We now investigate possible explanations for both the dependences on measured luminosity and the differences in the fit parameters. Note that multiplying the calculated luminosity by a constant factor changes both the intercept and the slope of the fits to the ratio.

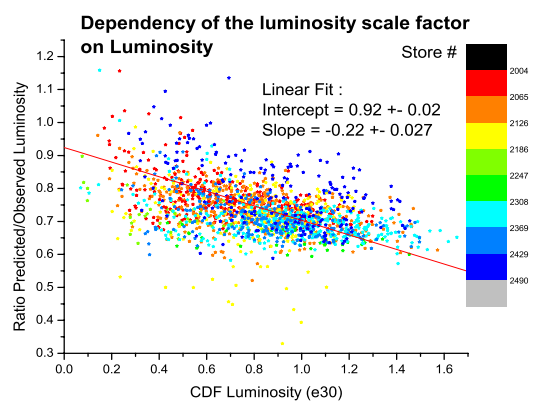

Figure 2 Ratio of calculated to measured CDF per bunch luminosity at the beginning of the store for a sample of 52 stores versus CDF luminosity.

We first consider the measured luminosities. Both CDF and D0 quote statistical errors of less than 1% and systematic errors of about ±5%. The ratio of the total D0 measured luminosity to that of CDF versus CDF luminosity is linear, with an intercept of 0.984±.001 and a slope of –0.00194±.00005. (At CDF luminosities of 20 and 40 10^{-30} cm^{-2} sec^{-1}, the ratio is 0.95 and 0.91 respectively.) This difference is enough to account for the difference between the D0 and CDF versions of the fits to the data in Figure 3 quoted above. Although there are significant store-to-store variations, within errors the

measured luminosities for CDF and D0 are linear with proton and anti-proton intensities, with no offset.

N_p and $N_{\bar{p}}$ have been calibrated to ±2%. H is not very sensitive to errors in σ_t and is quite constant for the data in Figures 2 and 3. For the data in Figure 2, the average H is .48±.02, and the average σ_t is 2.4±.4 ns for anti-protons and 2.5±.5 ns for protons. By definition, the $\beta*$ dependence is independent of luminosity. A larger than nominal $\beta*$ as indicated by the luminous region measurements reported above makes the disagreement slightly worse. If $\beta*$ were different at D0 than at CDF, it could help explain the differences between Fits 2 and 3. Most Tevatron experts believe the lattice parameters are only know to ±10%. These two factors could explain an intercept and slope factor of the order of ±10%.

The final factor in Equation 1 is the combination of emittances $F_{emit}=\sqrt{(\varepsilon_p+\varepsilon_{\bar{p}})_x(\varepsilon_p+\varepsilon_{\bar{p}})_y}$. A major difference between the data sets in Figures 2 and 3 is that the calculated luminosity uses the flying wire emittances in the first case and the synchrotron light emittances in the second case. There is direct evidence of a difference between the flying wire emittances and those measured by synchrotron light. Both measurements of emittances are recorded simultaneously at the beginning of each store. Comparing the ratios of emittances bunch by bunch over a large number of stores gives the relationships between the two methods shown in Table 2. However, this study gives no information as to whether either of them is correct. Preliminary beam scraping results give good agreement with proton vertical emittances and show significant discrepancies for the anti-proton vertical emittance measurements, in agreement with Table 2, indicating that the flying wire emittances are somewhat more reliable than the synchrotron light measurements. However, there is also evidence that the lattice parameters at the synchrotron light and flying wire locations are different from what is assumed in these calculations and could explain some of the inconsistencies.

The effective emittance is defined by solving Equation 1 for the factor F_{emit}. This can then be directly compared to $F_{emit,}$ evaluated with FW emittance measurements. For the same data as in Figure 2 averaged over all 36 bunches in the machine, the ratio of the FW F_{emit}. to the effective emittance is linear in measured luminosity with an intercept of 0.97±0.03 and a slope of –0.004±.001 For luminosities of 20 and 40 10^{30}cm^{-2}sec^{-1}, this translates into ratios of effective emittance to F_{emit} of .84-.94 and .74-.88 respectively. This result is very consistent with the ratio (.85) of the average effective emittance 19.6±2.9 and the average flying wires emittance factor 23.0±3.2 π mm mr evaluated for the same data.

DISCUSSION AND CONCLUSIONS

In this paper we have summarized current, as yet preliminary, understanding of the agreement between accelerator performance numbers as measured by Tevatron instrumentation compared to what is seen by the experiments. While there is qualitative agreement, much remains to be done. The different aspects of the comparisons need to be done on the same data sets. D0 is doing a luminous region study similar to that of CDF and both experiments are working on another method[7] of measuring the size of the luminous region in which the measurement resolution factors out, providing an important crosscheck. More scraping studies and better knowledge of the lattice parameters will help calibrate the flying wires and the synchrotron light. *We thank all members of the Sequenced Data Acquisition team for their dedicated support.*

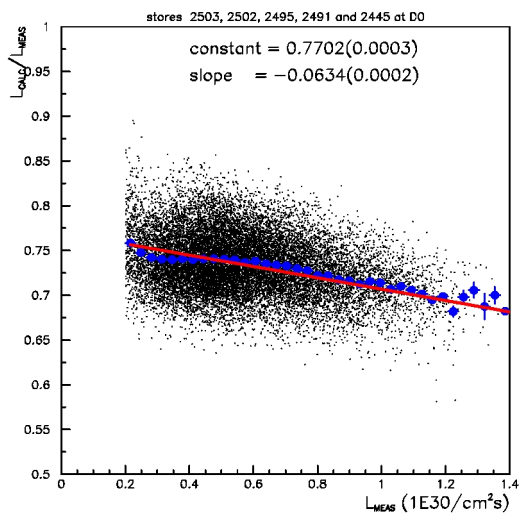

Figure 3 Ratio of calculated to measured D0 bunch-by-bunch luminosity during 5 stores versus D0 measured luminosity.

Table 2. Coefficients for the best linear fit formula for synchrotron light emittances (SL) in terms of the flying wire (FW) emittances (SL = Intercept + Slope*FW).

Quantity	Slope	Intercept
ε_x for protons	1.12±0.14	8.9±2.0
ε_y for protons	1.28±0.17	-0.5±4.7
ε_x for anti-protons	0.65±0.21	34.2±4.3
$\varepsilon_{y\ for}$ anti-protons	0.64±0.21	14.1±6.5

REFERENCES

1 D0 Collaboration, Fermilab_Conf-98/395-E, and for CDF, D. Acosta *et al.*, Nucl. Instrum. Meth. A **494**, 57 (2002).
2 M. Jones *et al,* Fermilab TM-2172.
3 G. Vogel *et al*, A Multi-Batch Fast Bunch Integrator for the Fermilab Main Ring
4 S. Pordes *et al*, Measurements of Proton and Antiproton beam intensities in the Tevatron' these proceedings
5 W. Blokland *et al*, A new Flying Wire System for the Tevatron, PAC`97.
6 H. Cheung, Performance of a Beam Monitor in the Fermilab Tevatron Using Synchrotron Light, these proceedings
7 L. Ristori *et al,* CDF Note 4189.